Published Ahead of Print on January 24, 2020 as 10.1212/WNL.0000000000009013

ARTICLE

Fat fraction distribution in lower limb muscles of patients with CMT1A

A quantitative MRI study

Joachim Bas, MD, Augustin C. Ogier, MSc, Arnaud Le Troter, PhD, Emilien Delmont, MD, PhD, Benjamin Leporq, PhD, Lauriane Pini, MSc, Maxime Guye, MD, PhD, Amandine Parlanti, MSc, Marie-Noëlle Lefebvre, MD, David Bendahan, PhD, and Shahram Attarian, MD, PhD

Correspondence
Dr. Attarian
sattarian@ap-hm.fr

Neurology® 2020;00:1-8. doi:10.1212/WNL.0000000000009013

Abstract

Objective

To quantitatively describe the MRI fat infiltration pattern of muscle degeneration in Charcot-Marie-Tooth (CMT) type 1A (CMT1A) disease and to look for correlations with clinical variables.

Methods

MRI fat fraction was assessed in lower-limb musculature of patients with CMT1A and healthy controls. More particularly, 14 muscle compartments were selected at leg and thigh levels and for proximal, distal, and medial slices. Muscle fat infiltration profile was determined quantitatively in each muscle compartment and along the entire volume of acquisition to determine a length-dependent gradient of fat infiltration. Clinical impairment was evaluated with muscle strength measurements and CMT Examination Scores (CMTESs).

Results

A total of 16 patients with CMT1A were enrolled and compared to 11 healthy controls. Patients with CMT1A showed a larger muscle fat fraction at leg and thigh levels with a proximal-to-distal gradient. At the leg level, the largest fat infiltration was quantified in the anterior and lateral compartments. CMTES was correlated with fat fraction, especially in the anterior compartment of leg muscles. Strength of plantar flexion was also correlated with fat fraction of the posterior compartments of leg muscles.

Conclusion

On the basis of quantitative MRI measurements combined with a dedicated segmentation method, muscle fat infiltration quantified in patients with CMT1A disclosed a length-dependent peroneal-type pattern of fat infiltration and was correlated to main clinical variables. Quantification of fat fraction at different levels of the leg anterior compartment might be of interest in future clinical trials.

From the Reference Center for Neuromuscular Diseases and ALS (J.B., E.D., A.P., S.A.) and CIC-CPCET (M.-N.L.), La Timone University Hospital, Aix-Marseille University; Aix-Marseille University (A.C.O., A.L.T., L.P., M.G., D.B.), CNRS, Center for Magnetic Resonance in Biology and Medicine; Aix-Marseille University (E.D.), UMR 7286, Medicine Faculty; Aix-Marseille University (S.A.), Inserm, GMGF; Aix Marseille University (A.C.O.), Université de Toulon, CNRS, LIS, Marseille; Université de Lyon (B.L.); and CREATIS CNRS UMR 5220 (B.L.), Inserm U1206, INSA-Lyon, UCBL Lyon 1, France.

Go to Neurology.org/N for full disclosures. Funding information and disclosures deemed relevant by the authors, if any, are provided at the end of the article.

Glossary

CMT = Charcot-Marie-Tooth; **CMTES** = CMT Examination Score; **CMTNSv2** = CMT Neuropathy Score Version 2; **CMT1A** = CMT type 1; **ONLS** = Overall Neuropathy Limitations Scale; **PDFF** = proton-density fat fraction; ***PMP22*** = peripheral myelin protein 22; **T1W** = T1-weighted.

Charcot-Marie-Tooth type 1A (CMT1A) is an autosomal dominant demyelinating polyneuropathy[1] (prevalence of ≈1 in 5,000[2]) associated with a DNA duplication located on the short arm of chromosome 17,[3] which contains the peripheral myelin protein 22 (*PMP22*) gene. The dysmyelination and abnormal interactions between myelin and axon occurring in CMT eventually lead to axonal loss, disability,[5] length-dependent motor deficits, and sensory symptoms.[4,5] Muscle atrophy and motor deficit arise in feet and legs and may follow later in the hands.

From a clinical endpoint, both the CMT Neuropathy Score Version 2 (CMTNSv2)[6] and the Overall Neuropathy Limitations Scale (ONLS) score have been validated for patients with CMT.[7] Given that CMT1A is a slowly progressive disease, sensitive outcome measures have been identified as the main issue for future clinical trials. Electrophysiologic studies have shown diffuse slowed nerve conduction velocity <38 m/s,[8] and Motor Unit Number Index has been reported as a potential biomarker of interest.[9] Skeletal muscle MRI has been used in CMT over the last 2 decades,[10] and quantitative approaches have been used only recently.[11–13] The corresponding metrics such as fat fraction have been quantified only in a single central slice for the leg. A good correlation with clinical severity and a high sensitivity to changes have been reported.[11,12]

In the present study, we intended to combine an MRI quantitative approach and a dedicated segmentation method to quantify fat fraction in 14 individual muscle compartments of the leg and thigh. The corresponding metrics were quantified in the whole set of MRI slices so that a potential proximal-to-distal gradient could be assayed. Correlations with electrophysiologic measurements and clinical scores were also analyzed.

Methods

Clinical assessment

Consecutive adult patients with CMT1A were included between March and November 2016 in the Reference Center for Neuromuscular Disease and ALS (Marseille-France) after informed consent was obtained. Clinical assessment included demographic characteristics, medical history, and neurologic examination. Muscle strength was assessed through manual testing with the Medical Research Council scale, and the 10-m walking test was performed.[14] Patients were scored with the CMT Examination Score (CMTES), a 12-point functional rating scale that incorporates both patient symptoms and examination findings.[15] Disease severity was determined on the basis of the CMTNSv2, a composite score comprising symptoms, signs, and neurophysiologic tests.[6] Limitations in daily activities were assessed with the ONLS.[16] Patients also had electrophysiologic assessment, including compound motor action potential and Motor Unit Number Index measurements on abductor pollicis brevis, abductor digiti minimi, and tibialis anterior nondominant muscles, as previously described.[9]

Genetic diagnosis was confirmed for all patients, and none of them had any other causes of neuropathy associated with CMT1A. The control group was composed of 11 individuals (5 female) with no medical history of neuromuscular disorder.

MRI studies

MRI was performed at 1.5T with a Siemens Avanto (Munich, Germany) scanner. Patients lay supine in the scanner, and the leg and thigh were imaged on the nondominant side with a combination of flexible coils on the top and a spine coil integrated into the scanner bed. After a localizer set of images, T1-weighted (T1W) and 3D gradient recalled echo sequences were recorded in the transverse plane over a 20-cm central area in both the leg and thigh with bony landmarks used to position the central slice. The corresponding parameters were repetition time/echo time of 549/11 milliseconds, 20 slices, slice thickness of 5 mm, and voxel size of 0.7 × 0.7 mm for the T1W sequence and repetition time/echo time of 22/2.38 to 19.06 milliseconds with a 2.38-millisecond step, 36 slices, slice thickness of 5 mm, and voxel size of 1.7 × 1.7 mm for the gradient recalled echo sequence.

Fat-water separation

The fat-water separation has been performed as previously described.[17] The proton-density fat fraction (PDFF) was calculated for each voxel as the ratio between the fat proton density and the sum of water and fat proton densities.

Supervised muscle segmentation

Regions of interest were manually drawn on T1W images (26) by an experienced physician (J.B., with >5 years of experience) using FSLView (FSL, FMRIB Software Library, Oxford, UK).[18] A total of 14 muscle groups were selected, 10 at the thigh level (rectus femoris, vastus lateralis, vastus medialis, vastus intermedius, sartorius, gracilis, semitendinosus, semimembranosus, biceps femoris, and adductor muscles) and 4 at the leg level (anterior, lateral, posterior deep, and posterior superficial). Regions of interest were manually segmented in a few slices, and segmentation of the missing slices was performed automatically along the longitudinal axis, as previously described.[19] Segmentation results were double-checked by 2 experts (J.B. and E.D.).

Table 1 Clinical characteristics of patients

Age, y	36.8 ± 15.0
Sex ratio, n	1:1
Disease duration, y	25.9 ± 14
Functional scores	
CMTNSv2	13.1 ± 3.6
CMTES	9.4 ± 2.5
ONLS	3.3 ± 1.1
Plantar flexion strength (MRC scale)	3.7 ± 1.3
Dorsiflexion strength (MRC scale)	3.8 ± 0.4
Fingers abduction strength (MRC scale)	3.8 ± 0.6
10 m walk test, s	7.0 ± 1.2

Abbreviations: CMTES = Charcot-Marie-Tooth Examination Score; CMTNSv2 = Charcot-Marie-Tooth Neuropathy Score Version 2; MRC = Medical Research Council; ONLS = Overall Neuropathy Limitations Scale.
Data are expressed as mean ± SD.

Quantitative data extraction

Regarding the extraction of quantitative data, PDFF maps were linearly resliced to the resolution of the T1W image. For each muscle, PDFF values were calculated as the average over all the voxels from these quantitative maps within the whole 3D region of interest and within each slice. To assay the gradient along the longitudinal axis, slices were gathered as central (2–4 central slices, depending on the muscle length), proximal (2–4 proximal slices), and distal (2–4 distal slices).

Statistical analysis

Statistical analyses were performed with Addinsoft Xlstat (version 2018.7). Values are presented as mean ± SD and were compared with nonparametric Wilcoxon-Mann-Whitney tests given the nongaussian distribution of the data. The Spearman rank correlation was used to analyze the correlations between metrics (r, Spearman ρ). Differences were considered significantly different at $p < 0.05$.

Data availability

All deidentified data and related documentation from this study are available on request to qualified researchers with no time limit, subject to a standard data-sharing agreement.

Standard protocol approvals, registrations, and patient consents

This research protocol was approved by our local ethics committee (Institutional Review Board No. 2015-A00799-40).

Results

Demographics and clinical description of patients

Among the 24 patients with CMT1A screened, 16 (8 female) were included and 8 patients were excluded because of the presence of an orthopedic prosthesis at the level of lower limbs. The selected patients had a typical clinical history with length-dependent neuropathy, muscle atrophy, and foot deformities predominantly in the distal extremities of the lower limbs. The first signs mostly appeared during childhood or adolescence, and similar cases were reported in most patients' families. The mean age (SD) was 36.8 (15.0) years, and the average duration of the disease was 25.9 (14.0) years. In healthy controls, the mean age was 42.6 (14.3) years, and the age and sex distributions were similar to those of controls ($p > 0.05$).

Clinical scores such as CMTNSv2, CMTES, and ONLS are summarized in table 1, together with muscular testing and results of the 10-m walk test.

MRI measurements

Visual analysis of T1W images illustrated a variable fatty infiltration at the leg level. The anterior and lateral compartments were the most frequently affected (69% and 62%, respectively), together with the gastrocnemius medialis muscle (62%). The soleus (37%), gastrocnemius lateralis (25%), and deep posterior compartment (17%) were less

Table 2 Proton-density fat fractions in individual muscles of controls and patients

Muscle	Controls (mean ± SD), %	Patients (mean ± SD), %	*p* Value
Leg muscle compartments			
Anterior	4.8 ± 1.7	17.7 ± 9.1	6.7×10^{-5}
Lateral	7.5 ± 2.8	21.8 ± 14.1	1.2×10^{-3}
Posterior deep	5.0 ± 2.3	11.2 ± 3.5	8.5×10^{-6}
Posterior superficial	5.5 ± 2.5	10.4 ± 6.0	0.01
Thigh muscle compartments			
Rectus femoris	5.3 ± 3.0	9.5 ± 6.6	0.04
Vastus lateralis	5.8 ± 2.7	7.9 ± 4.0	0.10
Vastus medialis	3.9 ± 1.8	6.5 ± 3.8	0.03
Vastus intermedius	4.1 ± 2.2	7.9 ± 6.0	0.03
Sartorius	9.6 ± 5.5	14.6 ± 7.3	0.05
Gracilis	7.5 ± 4.5	13.5 ± 7.9	0.01
Semitendinosus	6.0 ± 3.2	10.9 ± 5.1	0.01
Semimembranosus	6.2 ± 3.8	11.3 ± 6.2	0.01
Biceps femoris	6.5 ± 2.8	10.2 ± 5.2	0.03
Adductor muscles	6.7 ± 4.0	8.5 ± 4.3	0.28

Data are expressed in percent of fat infiltration as mean ± SD.

Figure 1 (A–D) PDFF expressed in percent in patients with Charcot-Marie-Tooth type 1 and controls

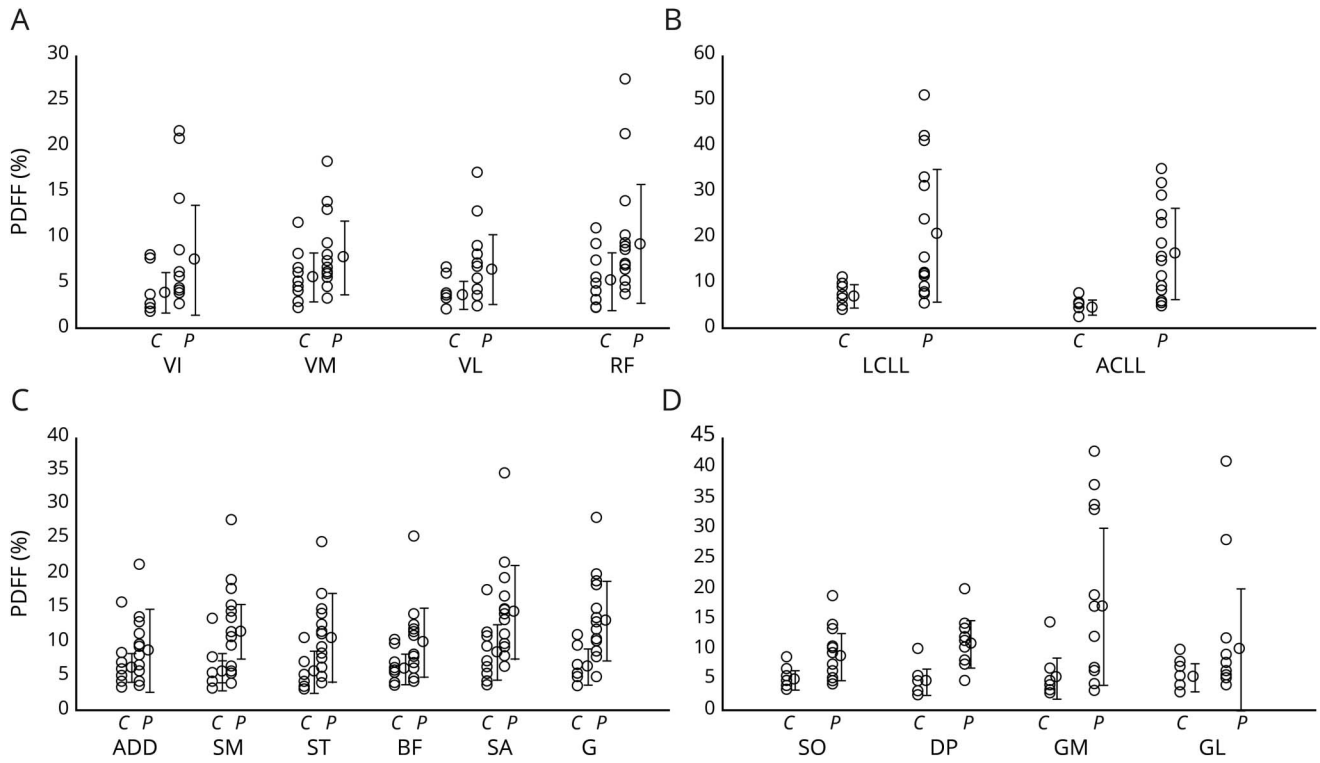

Values are presented as single measurements (each point) with mean values and SD as error bars. ACLL = anterior compartment of the lower leg; ADD = adductor muscles; BF = biceps femoris; C = control; G = gracilis; GL = gastrocnemius lateralis; GM = gastrocnemius medialis; LCLL = lateral compartment of the lower leg; OP = deep posterior compartment; P = patient; PDFF = proton density fat faction; RF = rectus femoris; SA = sartorius; SM = semimembranosus; SO = soleus; ST = semitendinosus; VJ = vastus intermedius; VL = vastus lateralis; VM = vastus medialis.

frequently affected. Visual analysis of T1W images at the thigh level showed minimal or no abnormalities. T1W images appeared normal at the leg and thigh levels in controls.

As indicated in table 2, the quantitative analysis clearly disclosed that muscular fat fraction was largely and significantly increased in patients with CMT1A compared to controls and for most leg (figure 1) and thigh muscle compartments. At the leg level, the largest fat fraction was quantified in the anterior and lateral compartments (268.8% and 190.7%, respectively, between patients and controls, vs 124.0% and 89.1% in the deep posterior and superficial posterior compartments). In patients, fat infiltration was significantly larger ($p < 0.05$) for the anterior and lateral compartments compared to the posterior ones (figure 1). At the thigh level, fat infiltration was milder and ranged from 26.9% (adductor muscles) to 92.7% (rectus femoris muscle). The detailed segmentation performed for the whole set of slices disclosed a fat infiltration gradient between the proximal and median slices ($p < 0.05$) and between the median and distal slices ($p < 0.05$) for leg muscles. At the thigh level, a proximal-to-distal fat infiltration was also observed (figure 2).

Regarding individual muscle volumes, significant muscular atrophy was observed in patients for most muscle compartments at both the leg and thig levels (table 3).

Correlations were studied between quantitative fat fraction, clinical scores, and electrophysiology measurements. For the leg muscle compartments and as indicated in table 4, fat

Figure 2 Length-dependent fat fraction gradient

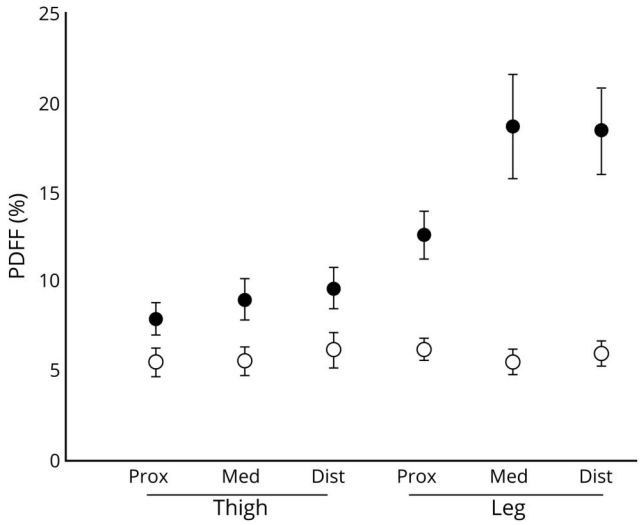

Muscle proton-density fat fraction (PDFF) increases from the proximal (Prox) to distal (Dist) segments for both leg and thigh levels ($p < 0.05$), thereby showing a length-dependent fat fraction gradient. Med = medial.

Table 3 Individual muscle volumes for controls and patients

Muscle	Controls (mean ± SD), cm^3	Patients (mean ± SD), cm^3	*p* Value
Leg muscle compartments			
Anterior	8.5 ± 4.3	6.7 ± 4.0	0.28
Lateral	19.9 ± 11.0	5.7 ± 2.0	1×10^{-4}
Posterior deep	13.5 ± 5.9	7.5 ± 4.5	0.01
Posterior superficial	10.9 ± 5.1	6.0 ± 3.2	0.01
Thigh muscle compartments			
Rectus femoris	14.6 ± 7.3	9.6 ± 5.5	0.05
Vastus lateralis	6.5 ± 3.8	3.9 ± 1.8	0.03
Vastus medialis	16.0 ± 5.2	10.2 ± 3.3	1.8×10^{-3}
Vastus intermedius	7.4 ± 4.2	4.6 ± 2.1	0.03
Sartorius	11.3 ± 6.2	6.2 ± 3.8	0.01
Gracilis	10.1 ± 10	6.0 ± 2.9	0.14
Semitendinosus	7.9 ± 6.0	4.1 ± 2.2	0.03
Semimembranosus	8.7 ± 4.0	5.3 ± 2.0	0.01
Biceps femoris	57.0 ± 10.1	48.0 ± 10.9	0.04
Adductor muscles	10.1 ± 4.9	6.5 ± 3.1	0.03

Data are expressed in cubic centimeters as mean ± SD.

fraction was significantly correlated with age and disease duration, whereas for the thigh compartments, a similar significant correlation was found only for disease duration. CMTES, $CMTNS_{lower\ limb}$, and $CMTNS_{lower\ limb\ motor}$ were significantly correlated with fat fraction computed in the medial leg muscle compartment (table 4). Regarding the thigh muscle compartments, a significant relationship was found between fat fraction and both CMTES and $CMTNS_{lower\ limb}$ (except for the distal compartment). Variables related to the 10-m walking test, that is, time and distance, were not correlated to fat fraction quantified in the leg muscle compartments. On the contrary, distance was correlated to fat fraction in the distal and medial thigh compartments (table 4). Dorsiflexion strength was not significantly correlated to fat fraction regardless of the muscle compartment. On the contrary, plantar flexion was significantly correlated to fat fraction of the whole set of leg and thigh compartments, that is, distal, proximal, and medial. Similarly, the motor unit size index was also correlated to the fat fraction computed for the whole set of leg and thigh compartments.

Discussion

In the present study, on the basis of quantitative MRI measurements combined with a dedicated segmentation method, the fat fraction pattern regarding individual muscles was reported in 16 patients with CMT1A at the thigh and leg levels. Multiple correlations with several clinical metrics were identified. These results further confirmed those from previous studies[11,13,20] and confirmed the interest of outcome measures provided by quantitative muscle MRI for future CMT clinical trials. In addition, our results extended the quantitative muscle MRI analysis to a larger volume of interest, that is, multiples slices and entire individual muscle volumes, thereby illustrating the pattern of muscle degeneration in patients with CMT1A and the existence of a proximal-to-distal gradient for multiple MRI variables.

Over the past 20 years, multiple MRI results have been reported in patients with CMT. On the basis of a visual analysis of T1W images, Stilwell et al.[10] illustrated the length-dependent nature of these neuropathies, showing a larger muscle degeneration in distal locations. Gallardo et al.[21] reported a selective involvement of intrinsic foot muscles and a distally accentuated fatty infiltration of the lateral, anterior, and superficial posterior leg muscle compartments and, to a lesser degree, of the deep posterior compartment in patients with CMT1A. More recently, a prevalent fatty infiltration in the anterior and lateral compartments was also reported.[22] These studies were based on a semiquantitative Goutallier classification,[23] which has been stated to be poorly sensitive in follow-up study.[24]

Based on a more quantitative approach and taking advantage of a dedicated segmentation protocol, our results further supported such a pattern of muscle degeneration that was predominant in the anterior and lateral compartments of the leg muscles with a length dependence. Indeed, the quantitative analysis of fat fraction in individual muscles of patients with CMT1A showed significantly increased values especially in the anterior and lateral leg muscle compartments compared to the posterior compartments, whereas such a difference was not observed in the control group. This quantitative analysis further supports the commonly reported CMT phenotype corresponding to a neuropathy affecting primarily peroneal muscles.[25] The comparative analysis of muscle fat fraction at different levels illustrated a length-dependent gradient with a larger muscle degeneration quantified distally in both thigh and leg muscles. Such a gradient was not observed in the control group and tended to increase with disease severity. When we consider moderately affected patients, that is, with a CMTNSv2 score below the 5th percentile, the mean muscle fat fraction at thigh level (i.e., proximally) was included in the 25th to 75th interquartile range of the control group. On the contrary, for severely affected patients, that is, those with a CMTNSv2 score above the 95th percentile, the fat fraction was in the 75th to 95th interquartile range of the control group. This proximal-to-distal gradient of muscle fatty infiltration has previously been suggested on the basis of semiquantitative MRI measurements[10,21] and further confirms the length-dependent degeneration of motor axons leading to muscle denervation in CMT1A.

Table 4 Significant *r* values for the correlations between fat fraction and other variables for the total leg and thigh muscle compartments

	Leg muscle compartments			Thigh muscle compartments		
	D	M	P	D	M	P
Age	*0.70*	*0.69*	*0.54*			
Disease duration	*0.75*	*0.69*	*0.60*	0.52	0.58	0.59
Clinical scores						
CMTNSv2						
CMTES		*0.56*		0.56	0.55	0.58
CMTNS lower limb		*0.58*			0.57	0.53
CMTNS lower limb motor		*0.65*	*0.67*			
Walking capacity						
Time						
Distance				0.60	0.54	
Force capacity						
Plantar flexion	*−0.83*	*−0.87*	*−0.87*	−0.57	−0.73	−0.68
Dorsiflexion						
Electrophysiology						
MUSIX tibialis anterior	*0.66*	*0.57*	*0.58*	0.58	0.62	0.64
MUNIX tibialis anterior						

Abbreviations: CMTES = Charcot-Marie-Tooth Examination Score; $CMTNS_{lower\ limb}$ = Charcot-Marie-Tooth Neurologic Score computed for the lower limb; $CMTNS_{lower\ limb\ motor}$ = Charcot-Marie-Tooth Neurologic Score computed for the lower limb and regarding the motor aspect; CMTNSv2 = Charcot-Marie-Tooth Neuropathy Score Version 2; D = distal; M = medial; MUSIX = Motor Units Size Index; MUNIX = Motor Unit Number Index; P = proximal.
Other variables include clinical scores, electrophysiology measurements, and strength.

Outcome measures should be considered for their responsiveness but also with respect to potential correlations with clinical, electrophysiologic, and functional parameters. Quantitative MRI has been used more recently in patients with CMT1A.[11,20,26] Sinclair et al.[13] reported a correlation between a composite mean lower-leg magnetization transfer ratio measure determined on a single central slice and the strength of ankle plantar flexion and disease duration. More recently, Morrow et al.[11,20] reported that the whole-muscle fat fraction measured for a single slice located at the midcalf was correlated with CMTES, disease duration, and the total Medical Research Council lower limb score. The larger sensitivity of this biomarker was underlined by the fact that muscle fat fraction increased significantly over a 1-year period, whereas clinical endpoints did not. These data were further confirmed in other groups of adult[20] and children[27] with CMT1A. In our group, similar results were observed; fat fraction was correlated to CMTES score and strength of plantar flexion. However, our results are more than confirmatory. Indeed, according to our multislice measurements, correlation coefficients at the leg level were the largest for the anterior compartment. In this anterior compartment, correlations were also observed at all slice levels—proximal, medial, and distal—and the whole set of slices, whereas the corresponding correlations were significant only at midcalf for the whole set of muscles, thereby highlighting the selectivity of muscle degeneration in CMT1A. The analysis of data from a single slice at the thigh and calf levels with only small regions of interest has been acknowledged as a limitation by Morrow et al.,[11] given that these measures might not account for the inhomogeneity of the disease. On the basis of an overall segmentation of different muscles compartments, a pattern of muscle degeneration has been characterized in CMT1A with a peroneal-type and length-dependent profile. Coefficient correlations with clinical metrics were high for the anterior compartment of leg muscles, so attention could be paid to these muscles in any future clinical trials.

In the present study, using quantitative MRI measurements combined with a dedicated segmentation method, we described the quantitative MRI pattern of muscle fatty degeneration in individual muscles of patients with CMT1A. The length-dependent peroneal-type profile of fat infiltration was further illustrated. Significant correlations between these metrics and main clinical variables were reported. Quantification of fat fraction at different levels of the leg anterior compartment appears to be of interest in future clinical trials.

Study funding

Funded by Centre National de la Recherche Scientifique (UMR 7339) and Assistance Publique Hôpitaux de Marseille.

Disclosure

The authors report no disclosures relevant to the manuscript. Go to Neurology.org/N for full disclosures.

Publication history

Received by *Neurology* July 28, 2020. Accepted in final form October 10, 2020.

Appendix Authors

Name	Location	Role	Contribution
Joachim Bas, MD	Reference Center for Neuromuscular Diseases and ALS, La Timone University Hospital, Aix-Marseille University, France	Author	Designed and conceptualized study; analyzed the data; performed statistical analysis; drafted the manuscript for intellectual content
Augustin C. Ogier, MSc	Aix-Marseille University, CNRS, Center for Magnetic Resonance in Biology and Medicine, UMR 7339, France	Author	Major role in the postprocessing of data; drafted the manuscript for intellectual content
Arnaud Le Troter, PhD	Aix-Marseille University, CNRS, Center for Magnetic Resonance in Biology and Medicine, UMR 7339, France	Author	Major role in the postprocessing of data; revised the manuscript for intellectual content
Emilien Delmont, MD, PhD	Reference Center for Neuromuscular Diseases and ALS, La Timone University Hospital, Aix-Marseille University, France	Author	Revised the manuscript for intellectual content
Benjamin Leporq, PhD	Université de Lyon; CREATIS CNRS UMR 5220, Inserm U1206, INSA-Lyon, UCBL Lyon 1, France	Author	Major role in the postprocessing of data
Lauriane Pini, MSc	Aix-Marseille University, CNRS, Center for Magnetic Resonance in Biology and Medicine, UMR 7339, France	Author	Major role in the acquisition of data
Maxime Guye, MD, PhD	Aix-Marseille University, CNRS, Center for Magnetic Resonance in Biology and Medicine, UMR 7339, France	Author	Revised the manuscript for intellectual content
Amandine Parlanti, MSc	Reference Center for Neuromuscular Diseases and ALS, La Timone University Hospital, Aix-Marseille University, France	Author	Major role in the postprocessing of data
Marie-Noëlle Lefebvre, MD	CIC-CPCET, La Timone University Hospital, Aix-Marseille University, Marseille, France	Author	Major role in acquisition of data
David Bendahan, PhD	Aix-Marseille University, CNRS, Center for Magnetic Resonance in Biology and Medicine, UMR 7339, France	Author	Designed and conceptualized study; supervised statistical analysis; revised the manuscript for intellectual content
Shahram Attarian, MD, PhD	Reference Center for Neuromuscular Diseases and ALS, La Timone University Hospital, Aix-Marseille University, France	Author	Design and conceptualized study; analyzed the data; revised the manuscript for intellectual content

References

1. Szigeti K, Lupski JR. Charcot-Marie-Tooth disease. Eur J Hum Genet 2009;17:703–710.
2. Barreto LC, Oliveira FS, Nunes PS, et al. Epidemiologic study of Charcot-Marie-Tooth disease: a systematic review. Neuroepidemiology 2016;46:157–165.
3. Lupski JR, de Oca-Luna RM, Slaugenhaupt S, et al. DNA duplication associated with Charcot-Marie-Tooth disease type 1A. Cell 1991;66:219–232.
4. Pareyson D, Marchesi C. Natural history and treatment of peripheral inherited neuropathies. Adv Exp Med Biol 2009;652:207–224.
5. Colomban C, Micallef J, Lefebvre MN, et al. Clinical spectrum and gender differences in a large cohort of Charcot-Marie-Tooth type 1A patients. J Neurol Sci 2014;336:155–160.
6. Murphy SM, Herrmann DN, McDermott MP, et al. Reliability of the CMT neuropathy score (second version) in Charcot-Marie-Tooth disease. J Peripher Nerv Syst 2011;16:191–198.
7. Mandel J, Bertrand V, Lehert P, et al. A meta-analysis of randomized double-blind clinical trials in CMT1A to assess the change from baseline in CMTNS and ONLS scales after one year of treatment. Orphanet J Rare Dis 2015;10:74.
8. Manganelli F, Pisciotta C, Reilly MM, et al. Nerve conduction velocity in CMT1A: what else can we tell? Eur J Neurol 2016;23:1566–1571.
9. Bas J, Delmont E, Fatehi F, et al. Motor Unit Number Index correlates with disability in Charcot-Marie-Tooth disease. Clin Neurophysiol 2018;129:1390–1396.
10. Stilwell G, Kilcoyne RF, Sherman JL. Patterns of muscle atrophy in the lower limbs in patients with Charcot-Marie-Tooth disease as measured by magnetic resonance imaging. J Foot Ankle Surg 1995;34:583–586.
11. Morrow JM, Sinclair CD, Fischmann A, et al. MRI biomarker assessment of neuromuscular disease progression: a prospective observational cohort study. Lancet Neurol 2016;15:65–77.
12. Morrow JM, Sinclair CD, Fischmann A, et al. Reproducibility, and age, body-weight and gender dependency of candidate skeletal muscle MRI outcome measures in healthy volunteers. Eur Radiol 2014;24:1610–1620.
13. Sinclair CD, Morrow JM, Miranda MA, et al. Skeletal muscle MRI magnetisation transfer ratio reflects clinical severity in peripheral neuropathies. J Neurol Neurosurg Psychiatry 2012;83:29–32.
14. Graham JE, Ostir GV, Fisher SR, Ottenbacher KJ. Assessing walking speed in clinical research: a systematic review. J Eval Clin Pract 2008;14:552–562.
15. Shy ME, Blake J, Krajewski K, et al. Reliability and validity of the CMT neuropathy score as a measure of disability. Neurology 2005;64:1209–1214.
16. Graham RC, Hughes RA. A modified peripheral neuropathy scale: the Overall Neuropathy Limitations Scale. J Neurol Neurosurg Psychiatry 2006;77:973–976.
17. Leporq B, Lambert SA, Ronot M, Vilgrain V, Van Beers BE. Simultaneous MR quantification of hepatic fat content, fatty acid composition, transverse relaxation time and magnetic susceptibility for the diagnosis of non-alcoholic steatohepatitis. NMR Biomed Epub 2017 July 5.
18. Jenkinson M, Beckmann CF, Behrens TE, Woolrich MW, Smith SM. Fsl. Neuroimage 2012;62:782–790.
19. Ogier A, Sdika M, Foure A, Le Troter A, Bendahan D. Individual muscle segmentation in MR images: a 3D propagation through 2D non-linear registration approaches. Conf Proc IEEE Eng Med Biol Soc 2017;2017:317–320.
20. Morrow JM, Evans MRB, Grider T, et al. Validation of MRC Centre MRI calf muscle fat fraction protocol as an outcome measure in CMT1A. Neurology 2018;91:e1125–e1129.
21. Gallardo E, Garcia A, Combarros O, Berciano J. Charcot-Marie-Tooth disease type 1A duplication: spectrum of clinical and magnetic resonance imaging features in leg and foot muscles. Brain 2006;129:426–437.

22. Chung KW, Suh BC, Shy ME, et al. Different clinical and magnetic resonance imaging features between Charcot-Marie-Tooth disease type 1A and 2A. Neuromuscul Disord 2008;18:610–618.
23. Goutallier D, Postel JM, Bernageau J, Lavau L, Voisin MC. Fatty muscle degeneration in cuff ruptures: pre- and postoperative evaluation by CT scan. Clin Orthop Relat Res 1994;304:78–83.
24. Pelayo-Negro AL, Gallardo E, Garcia A, et al. Evolution of Charcot-Marie-Tooth disease type 1A duplication: a 2-year clinico-electrophysiological and lower-limb muscle MRI longitudinal study. J Neurol 2014;261:675–685.
25. Price AE, Maisel R, Drennan JC. Computed tomographic analysis of pes cavus. J Pediatr Orthop 1993;13:646–653.
26. Sinclair CD, Miranda MA, Cowley P, et al. MRI shows increased sciatic nerve cross sectional area in inherited and inflammatory neuropathies. J Neurol Neurosurg Psychiatry 2011;82:1283–1286.
27. Cornett KMD, Wojciechowski E, Sman AD, et al. Magnetic resonance imaging of the anterior compartment of the lower leg is a biomarker for weakness, disability, and impaired gait in childhood Charcot-Marie-Tooth disease. Muscle Nerve 2019;59:213–217.

Fat fraction distribution in lower limb muscles of patients with CMT1A: A quantitative MRI study

Joachim Bas, Augustin C. Ogier, Arnaud Le Troter, et al.

Neurology published online January 24, 2020
DOI 10.1212/WNL.0000000000009013